Photochemical & Photobiological Sciences

Dynamic Article Links

Cite this: *Photochem. Photobiol. Sci.*, 2012, **11**, 1428

www.rsc.org/pps

PAPER

Cell death response of U87 glioma cells on hypericin photoactivation is mediated by dynamics of hypericin subcellular distribution and its aggregation in cellular organelles

Veronika Huntosova,[a,b] Zuzana Nadova,[a] Lenka Dzurova,[a] Viera Jakusova,[c] Franck Sureau*[b] and Pavol Miskovsky*[a,d]

Received 16th December 2011, Accepted 25th May 2012
DOI: 10.1039/c2pp05409d

Hypericin (Hyp) is a hydrophobic natural photosensitizer that is considered to be a promising molecule for photodynamic treatment of tumor cells and photo-diagnosis of early epithelial cancers. Its hydrophobicity is the main driving force that governs its redistribution process. Low-density lipoproteins (LDL), a natural *in vivo* carrier of cholesterol present in the vascular system, have been used for targeted transport of Hyp to U87 glioma cells. For low Hyp–LDL ratios ($\leq$10 : 1), the cellular uptake of Hyp is characterized by endocytosis of the [Hyp–LDL] complex, while Hyp alone can enter cells by passive diffusion. Photo-induced cell death and the mitochondrial membrane potential, observed for glioma cells after various times of incubation with the [Hyp–LDL] complex or Hyp alone, were monitored by flow-cytometry analysis using Annexin-V-FITC propidium iodide and $DiOC_6(3)$ staining. Differences of the results are discussed in view of the respective dynamic subcellular distributions of the drugs that were obtained by co-localization experiments using confocal fluorescence microscopy. In order to give clear evidence of specific intracellular localization and to identify possible Hyp aggregation in cellular organelles, fluorescence resonance energy transfer (FRET) between selected fluorescent organelle probes and Hyp was also assessed. It is shown, that the observed photo-induced cell deaths can be correlated with the sub-cellular distribution of the active fluorescent monomer form of Hyp in lysosomes (as determined from steady-state fluorescence experiments), but that possible aggregation of Hyp in some organelles, as determined from FRET experiments, should be taken into account for interpretation of the real dynamics of the subcellular redistribution. Results of the present study underline the fact that photo-induced cell death processes are strongly influences by dynamics of Hyp subcellular redistribution processes involving monomer-aggregate equilibrium. Such an observation should be taken in consideration for further optimization of Hyp *in vivo* PDT applications.

Introduction

The photosensitizer hypericin (Hyp) is a natural occurring plant pigment historically used in folk medicine. In the last few decades, it became the subject of interest of photo-physical and photo-biological research. Hyp exhibits a number of potential pharmacological applications including antiviral activity, anti-depressant properties and others.[1] In the field of cancer therapy, two main potential medicinal applications of Hyp have been described: first, its photosensitizing activity has been characterized by high singlet oxygen production, minimal dark toxicity, tumor selectivity and high clearance rate from the host body that makes it a promising drug for application in PDT.[2–7] Secondly, its specific accumulation, observed in several types of tumor cells, can also be used for photo-diagnosis of early epithelial cancer.[8,9] The cell death mechanisms of Hyp following photo-activation have recently been reviewed.[1] However, the precise description of some relevant mechanisms of Hyp cellular photo-toxicity processes is still not complete. The sub-cellular localization and distribution of the photosensitizer play key roles for applications in PDT, since it is known that short lifetimes of photo-induced reactive oxygen species (ROS) limit their diffusion to a distance of a few nm. Consequently, there have been many attempts to determine the specific sub-cellular localization of Hyp in several cell lines.[10–16] Most of these studies denoted perinuclear localization, which was later defined more precisely

[a]*Department of Biophysics, University of Pavol Jozef Safarik, Kosice, Slovak Republic. E-mail: pavol.miskovsky@upjs.sk; Fax: +421 55 62 229 86; Tel: +421 55 62 229 86*
[b]*ANBioPhy, CNRS-FRE 3207, Pierre & Marie Curie University, Paris, France. E-mail: franck.sureau@upmc.fr; Fax: +33 1 44 27 47; Tel: +33 1 44 27 47 17*
[c]*Department of Public Health, Jessenius Faculty of Medicine in Martin, Comenius University, Martin, Slovak Republic*
[d]*Department of Biophotonics, International Laser Center, Bratislava, Slovak Republic*

as the locus of Golgi apparatus and endoplasmic reticulum.[17,18] Some other studies have described lysosomes as the potential Hyp subcellular target with regard to its specific binding with extra-cellular lipoproteins, especially LDL.[19] Hyp has also been reported to accumulate in mitochondria that are considered as a key sub-cellular locus for apoptotic process.[10,11,20,21] In all cases, the hydrophobic character of Hyp appears as the driving force for its cellular membrane attraction because of their lipid composition.[22] From our point of view, these different reported results might be explained by the fact that the intracellular distribution of Hyp is actually dependent (i) on the time of incubation, (ii) on the concentration of the drug, as well as (iii) on the delivery system.[19] Moreover, as shown in our previous work, the fluorescence intensity of Hyp is not in itself sufficient to determine its sub-cellular localization since a high intracellular concentration of Hyp leads to fluorescence quenching as a result of its aggregation.[23] Ritz *et al.* have previously reported such a Hyp fluorescence decrease in U373 MG cells[24] and Theodossiou *et al.* have already discussed possible aggregations of Hyp in PAM 212 murine keratinocytes.[25] Hence, selective accumulation of Hyp in some subcellular organelles, such as mitochondria, might be underestimated due to local aggregation. Moreover, dynamics of such an aggregation process will strongly influence the specific subcellular locus where photo-activation takes place.

Taking into account that (i) LDLs have been described as the natural *in vivo* delivery system of Hyp and that (ii) cancer cells (particularly glioma cancer cells) are characterized by over-expression of LDL-receptors in comparison with the normal cells,[26–28] the LDL endocytosis pathway should also play an important role in the cellular accumulation and subsequent sub-cellular distribution of Hyp.[29–33] Accordingly, we have observed that over-expression of the LDL receptors on the cellular cytoplasmic membrane leads to an increase in the intracellular accumulation of Hyp[19] and that, for a low Hyp–LDL ratio (10 : 1), the cellular uptake of Hyp is characterized by endocytosis of the [Hyp–LDL] complex.[19,23] Therefore, in this study, photo-induced cell death was monitored in U-87 MG glioma cells as a function of the incubation time with either free Hyp or with the [Hyp–LDL] complex (Hyp–LDL ratio 10 : 1). It should be noted that if the addition of free Hyp in the extra cellular medium leads to some aggregate formation in equilibrium, with very low Hyp monomer concentration, it does not preclude the fast cellular uptake of its monomer fluorescent form, since the very high affinity for cellular lipids membrane induces a fast displacement of the monomer–aggregate equilibrium.[23] Results of photo-induced cell death were compared and discussed in view of the respective dynamics of Hyp sub-cellular distribution as observed in fluorescence microscopy.

Materials and methods

Chemicals

Hypericin, low-density lipoproteins, MitoTracker® Green FM, LysoTracker® Green DND-26, ER-Tracker Green, NBD C_6-ceramide bound to bovine serum albumin (BSA), Dulbecco's modified Eagle's medium (D-MEM), fetal bovine serum (FBS), phosphate saline buffer (PBS), penicillin/streptomycin, sodium pyruvate, glucose and SYTOX Green were purchased from Gibco Invitrogen (France). Ultroser® G was purchased from Pall Life Sciences (France) and Annexin-V-FITC from Becton, Dickinson (Canada). $DiOC_6(3)$ and CCCP (carbonyl cyanide 3-chlorophenylhydrazone) were purchased from Sigma-Aldrich Co.

Cell culture

U87 glioma cells were grown in standard conditions: 10% bovine fetal serum (FBS), 1% penicillin/streptomycin, 1% sodium pyruvate and D-MEM medium containing L-glutamine and high glucose (4500 mg ml^{-1}). One day before experiment, culture medium was changed for 2% Ultroser® G medium, a serum substitute that is used to replace FBS in cell culture media in order to avoid a lipid depletion condition. Cells were seeded in Petri dishes or culture flasks at a density of 10^5 cells per 1 ml. All cultures were kept in dark condition, 5% CO_2 and 95% humid atmosphere.

Cells response to Hyp photo-activation

Cells were irradiated using a 600 nm (maximum of Hyp absorption) monochromatic homemade diode illuminator with 4 J cm^{-2} light dose. Cellular response was observed 24 h after irradiation and compare with non-treated cells keep in dark conditions (control).

Flow-cytometry

Cell death was monitored with standard Annexin-V-FITC (PS staining) and propidium iodide (PI) (DNA staining)[34] (BD Pharmingen™). Annexin-V-FITC (5 µl) and PI (5 µl) were added for 10^5 cells. Cells were then analyzed by MACSQuant® Analyzer (Miltenyi Biotec, Germany). The 488 nm line of Argon laser was used for excitation. Annexin-V-FITC fluorescence emissions were measured in FITC channel (channel B1, band pass filter 500–550 nm) and PI emission (λ_{max} 620 nm) was measured in PI/PE-Cy5 channel (channel B3, band pass filter 655–730 nm) to avoid contribution of Hyp red fluorescence (λ_{max} 600 nm). Early apoptotic cells are stained with Annexin-V-FITC only while late apoptotic or necrotic cells are both stained with PI and Annexin-V-FITC. The mitochondrial membrane potential $\Delta\Psi_m$ was monitored by selective accumulation of $DiOC_6(3)$, a membrane-permeant cationic lipophilic probe. $DiOC_6(3)$ (1 nM) was added to cells 5 min before analysis by MACSQuant® Analyzer (Miltenyi Biotec, Germany). Green emission of $DiOC_6(3)$ was measured in the FITC channel. Cells incubated with CCCP (50 µM) were used as a positive control for total depolarization of the mitochondrial membrane potential.[35]

Sub-cellular distribution

Cells were incubated for 1 h, 3 h, 6 h and 24 h with either 500 nM Hyp free in DMSO (<0.5%), or with previously solubilized 500 nM Hyp within LDLs (Hyp–LDL ratio 10 : 1). The specific fluorescent organelle probe was then added 15 min before measurements. Respective probe concentrations are 100 nM for MitoTracker® Green FM, 300 nM for LysoTracker® Green DND-26, 5 µM for NBD C_6-ceramide and 1 µM for

ER-Tracker™ Green. Cells were washed before observation by an epifluorescence microscope Optiphot-2 equipped with a Nipkow coaxial-confocal attachment (Technical Instrument). Fluorescence images were taken using a water-immersion objective (Zeiss, Neofluar, x63, N.A. 1.2), a TE cooled CCD camera (Micromax, Princeton Instruments) and standard filters system: FITC filter set for green fluorescence detection (λ_{exc} = 450–490 nm, λ_{em} = 520–570 nm) and rhodamine filter set for red fluorescence (λ_{exc} = 530–560 nm, λ_{em} > 600 nm). Acquisition time was set to 5 s. Image processing was performed by IPLab software (Scanalytics).

Co-localization analysis

Co-localization analysis was performed on fluorescence images obtained above using the Image J software and a special MBF Image J for Microscopy Collection developed by Tony Collins. Mander's coefficients, defined as follow, were used for co-localization analysis:[36]

$$M = (R_i \cdot G_i)/\sqrt{[\sum R_i^2 \sum G_i^2]} \quad (1)$$

$$M_{1\mathrm{Red}} = \sum (R_i \cdot G_i)/\sum R_i^2 \quad (2)$$

$$M_{2\mathrm{Green}} = \sum (R_i \cdot G_i)/\sum G_i^2 \quad (3)$$

Where R_i and G_i are the signal intensity of the pixel number "i" obtained for the red and the green channel, respectively. M-values are thus ranging from 0 to 1. Absolute co-localization corresponds to M = 1. As showed by Bolte and Cordelieres,[37] the $M_{1\mathrm{Red}}$ correlation coefficient, displays how well the red pixels co-localize with some green ones, and the $M_{2\mathrm{Green}}$ correlation coefficient displays how well the green pixels co-localize with some red ones. Overlap coefficient does not depend on the relative strengths of each channel, but can be affected by the background signal. Prior to co-localization analysis, all microscopy images were processed using the Richardson–Lucy deconvolution algorithm in order to eliminate blur and noise present in images. The point spread functions (PSF) used in deconvolution were extracted individually from each image using a method proposed by Boutet de Monvel *et al.*,[38] namely by cropping an approximate PSF directly from images considering the point-like structures within experimental images.

FRET experiments

Detection of the accumulation of Hyp in different organelles was monitored by FRET measurements between specific fluorescent organelle probes (donor) and Hyp (acceptor). Evidence for FRET was given by the decrease in the fluorescence lifetime of the donor (*i.e.* the organelle specific fluorescent probe). Time resolved fluorescence microscopy can be used in this prospect.[39] The frequency based lifetime measurement technique used in our studies was already described in our previous paper.[23] Two fluorescent organelle probes have been used: LysoTracker® Green DND-26 (to study Hyp localization in lysosome) and NBD C_6-ceramide (to study Hyp localization in Golgi apparatus). Co-localization experiments for mitochondria and endoplasmatic reticulum could not have been performed by FRET due to the very short lifetime of the corresponding organelle probes (<1 ns), which exceeded time resolution of the experimental set up.

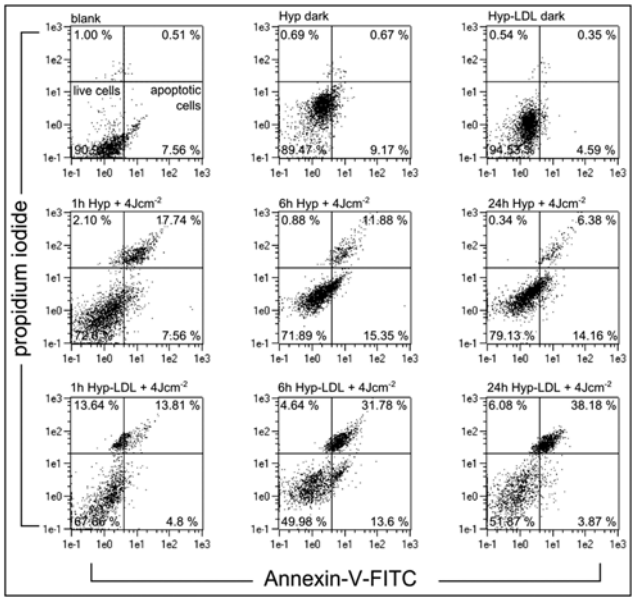

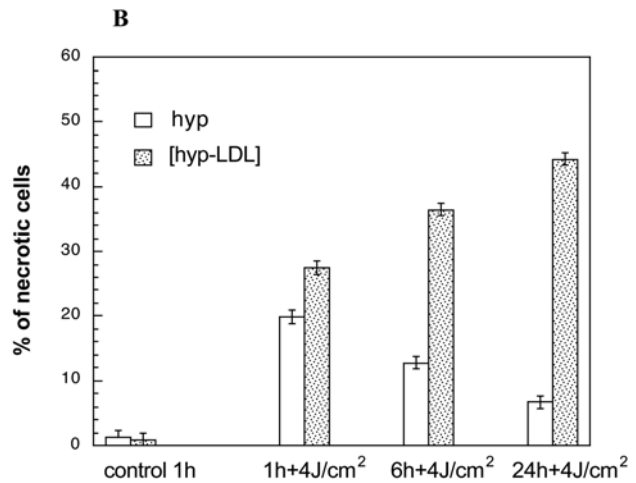

Fig. 1 (A) Flow-cytometric dot plot analysis of U87 glioma cells stained with propidium iodide and Annexin-V-FITC after incubation with Hyp (500 nM) or [Hyp–LDL] complex (Hyp–LDL ratio: 10 : 1, 500 nM Hyp). *First row*: blank - control cells, cells after 24 h incubation with Hyp (dark condition), cells after 24 h incubation with [Hyp–LDL] (dark condition). *Second row*: cells irradiated (600 nm, 4 J cm^{-2}) 1 h after incubation with Hyp and then observed 24 h after irradiation, cells irradiated (600 nm, 4 J cm^{-2}) 6 h after incubation with Hyp and then observed 24 h after irradiation, cells irradiated (600 nm, 4 J cm^{-2}) 24 h after incubation with Hyp and then observed 24 h after irradiation. *Third row*: cells irradiated (600 nm, 4 Jcm^{-2}) 1 h after incubation with [Hyp–LDL] and then observed 24 h after irradiation, cells irradiated (600 nm, 4 J cm^{-2}) 6 h after incubation with [Hyp–LDL] and then observed 24 h after irradiation, cells irradiated (600 nm, 4 J cm^{-2}) 24 h after incubation with [Hyp–LDL] and then observed 24 h after irradiation. (B) Corresponding histogram of necrotic cells (% of the total population).

Results and discussion

Cells response to Hyp photo-induced processes

U87 MG cells were irradiated at 600 nm (4 J cm^{-2}) after 1 h, 6 h or 24 h incubation with either Hyp or the [Hyp–LDL] complex. Photo-induced cell death was then further analyzed 24 h after irradiation by flow cytometry assessment (Fig. 1). For cells incubated with Hyp, photo-induction of cell death is rather limited and appears to be more efficient for shorter incubation times (20% necrotic cells for 1 h incubation) than for longer ones (respectively 13% and 7% for 6 h and 24 h incubation). On the other hand, photo-induced cell death is more pronounced for cells incubated with the [Hyp–LDL] complex and is increased along with the incubation time (respectively 27%, 36% and 44% for 1 h, 6 h and 24 h incubation). Accordingly, depolarization of the mitochondrial membrane ($\Delta\Psi_m$), which is one of the indicators of the apoptotic and necrotic cell death pathway, is not observed for cells treated with Hyp alone.[40] Hyper-polarization can even be observed for cells irradiated after 1 h incubation. Such hyper-polarization can be interpreted as the result of anti-apoptotic responses of the cells. On the other hand, photo-induced mitochondrial depolarization increases along with the incubation time for cells treated with the [Hyp–LDL] complex (Fig. 2). Thus, for quite low irradiation levels (4 J cm^{-2}), cellular delivery of Hyp by LDL appears to increase photo-induced cell death.

Intracellular localization of Hyp – co-localization experiments

Localization of Hyp in U87 MG cells was studied by steady-state fluorescence imaging with co-localization analysis. Extracellular medium with Ultroser-G instead of bovine fetal serum was used in order to avoid competitive entrapment of Hyp in the lipid phase of the serum. Under these conditions, a rapid cellular uptake of Hyp is observed after 1 h incubation with 500 nM Hyp (Fig. 3a–c). Fig. 3a illustrates the efficiency of the co-localization analysis method:[36] a diffuse correlation plot with low values of all Mander's coefficients are observed, which reflects that the actual absolute non co-localization of the two organelle specific fluorescent probes (Lysotracker Green for lysosome staining and the Mitotracker Red for mitochondrial staining). Fig. 3b and corresponding Table 1 represent the results of the co-localization analysis of Hyp in mitochondria, lysosome, Golgi apparatus and endoplasmic reticulum respectively obtained after 1 and 24 h of incubation with either Hyp or the [Hyp–LDL] complex. From a general point of view it is clear that intracellular Hyp staining is not limited to a specific compartment since M_{2green} values obtained for cells stained with the different organelle specific fluorescent probes are all equal or close to 1. This means that some Hyp fluorescence can be observed in all subcellular organelle. However, M_{1red} allows us to determine in which organelle the fluorescence of Hyp is the most pronounced. Actually, one hour after incubation, relative distribution of free Hyp appears to be mainly localized within lysosome (M_{1red} = 0.83) and endoplasmic reticulum (M_{1red} = 0.89) and to a much less extent within the mitochondria (M_{1red} = 0.42) and Golgi apparatus (M_{1red} = 0.3). The situation is quite different for cells incubated with the [Hyp–LDL] complex since, after one hour of incubation, Hyp appears to be mainly located in the mitochondria (M_{1red} = 0.93) and endoplasmic reticulum (M_{1red} = 0.95) and to a less extent in lysosome (0.53) and Golgi apparatus (M_{1red} = 0.49). Thus, after 1 h of incubation, the main significant difference is that preferential lysosomial fluorescence is observed for cells incubated with free Hyp while preferential mitochondrial fluorescence is observed for cells incubated with the [Hyp–LDL] complex. This situation is changed after 24 h of incubation: for cells incubated with free Hyp, mitochondrial staining is increased (M_{1red} = 0.98 instead of 0.42), lysosomial and Golgi apparatus staining are decreased (respectively, M_{1red} = 0.62 instead of 0.83 and M_{1red} = 0.14 instead of 0.3) and endoplasmic reticulum staining is not significantly changed (M_{1red} = 0.93 instead of 0.89). For cells incubated with the [Hyp–LDL] complex, lysosomial staining is increased (M_{1red} = 0.79 instead of 0.53), mitochondrial and Golgi apparatus staining are decreased (respectively, M_{1red} = 0.79 instead of 0.93 and M_{1red} = 0.33 instead of 0.49) and endoplasmic reticulum staining is not significantly changed (M_{1red} = 0.98 instead of 0.95). Thus,

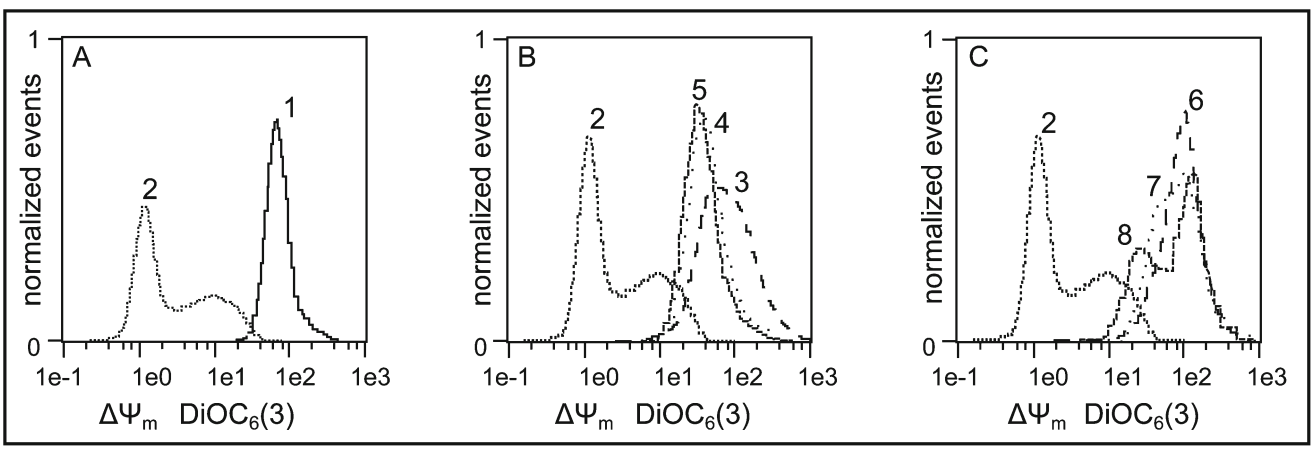

Fig. 2 Assessment of the mitochondrial membrane potential ($\Delta\Psi_m$) of U87 MG cells 24 h after irradiation (600 nm, 4 J cm^{-2}). Flow-cytometric histograms of the $DiOC_6(3)$ fluorescence correspond to: (1) Control cells, (2) cells incubated with CCCP, (3) cells incubated for 1 h with Hyp before irradiation (4) cells incubated for 6 h with Hyp before irradiation, (5) cells incubated for 24 h with Hyp before irradiation, (6) cells treated 1 h with [Hyp–LDL] before irradiation, (7) cells treated 6 h with [Hyp–LDL] before irradiation, (8) cells treated 24 h with [Hyp–LDL] before irradiation.

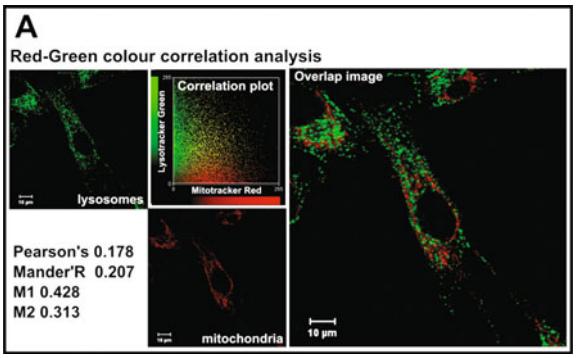

Fig. 3a Illustration of the method used for co-localization analysis of specific organelle probes with Hyp in U87 glioma cells by microscopic fluorescence imaging. U87 MG cells were stained both with the lysosomal fluorescence probes Lysotracker Green (image in green) and with the mitochondrial fluorescence probes Mitotracker Red (image in red). Correlation plot of red and green pixels of the images and overlap image (right) are also presented. Pearsons, Mandersons co-localization coefficients were calculated from these two images (see Materials and methods). *M* values give evidences for non-co-localization of these two probes and display their respective specificity for lysosomes and mitochondria.

between 1 and 24 h, the preferential intracellular fluorescence localization of Hyp is apparently going in two opposites ways: for cells incubated with free Hyp, transfer of fluorescence from lysosome (and Golgi apparatus) to mitochondria is observed while for cells incubated with the [Hyp–LDL] complex, transfer of fluorescence from mitochondria (and Golgi apparatus) toward lysosomes is observed. However, it should be noted that the absence of Hyp fluorescence (drug accumulation) in lysosomes for cells after 1 h of incubation with [Hyp–LDL], does not appear to be in agreement with the specific cellular uptake of LDL by the endocytosis pathway. As we have previously reported, accumulation of Hyp in some organelles could lead to the formation of non-fluorescent aggregates as revealed by the decrease of its intracellular fluorescence lifetime (from 7.5 ns down to 2 ns), due to FRET from Hyp monomers to aggregates.[23] This could result in incorrect interpretation of fluorescents co-localization images. Hence, non-fluorescent aggregate formation of Hyp should be taken into account to determine the actual intracellular traffic of Hyp. To overcome such an artifact, we have taken advantage of possible FRET between lysotracker green (a specific organelles probes that can act as donor) and Hyp molecules (that can act as acceptor even when

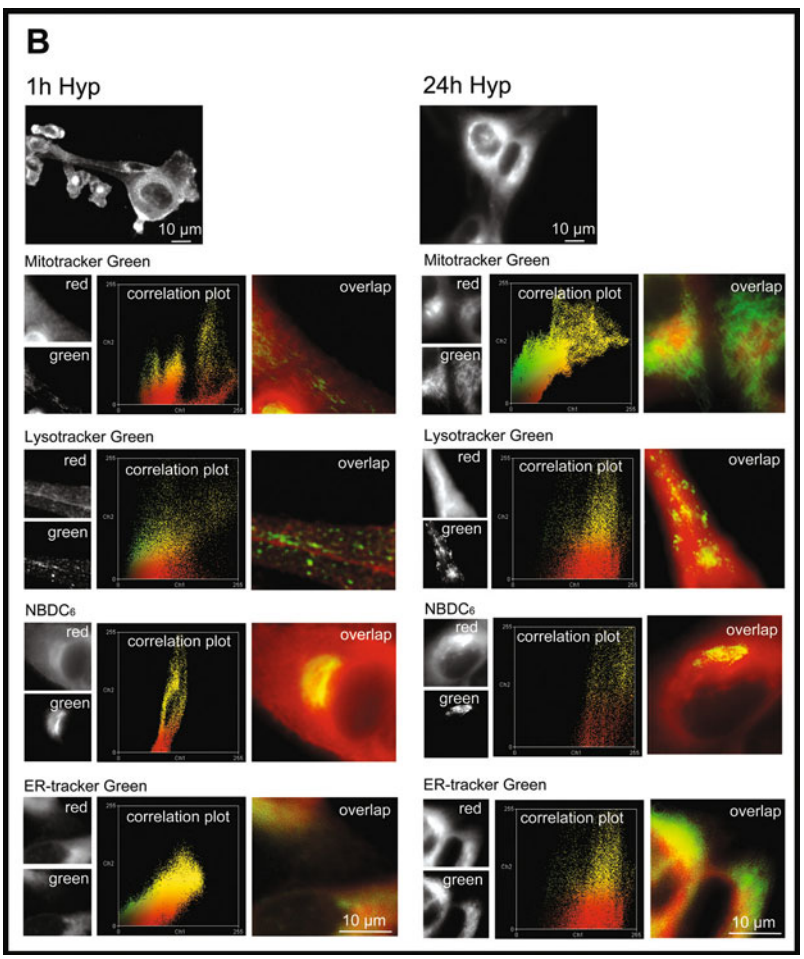

Fig. 3b Fluorescence images of U87 MG cells stained with specific fluorescent organelle probes (Mitotracker for mitochondria, Lysotracker for lysosomes, $NBDC_6$ for Golgi apparatus and ER-tracker for endoplasmic reticulum) were obtained after 1 h or 24 h incubation with free Hyp. Correlation plots, between Hyp red fluorescence and green fluorescence of each organelle probe, are given as well as corresponding overlap images.

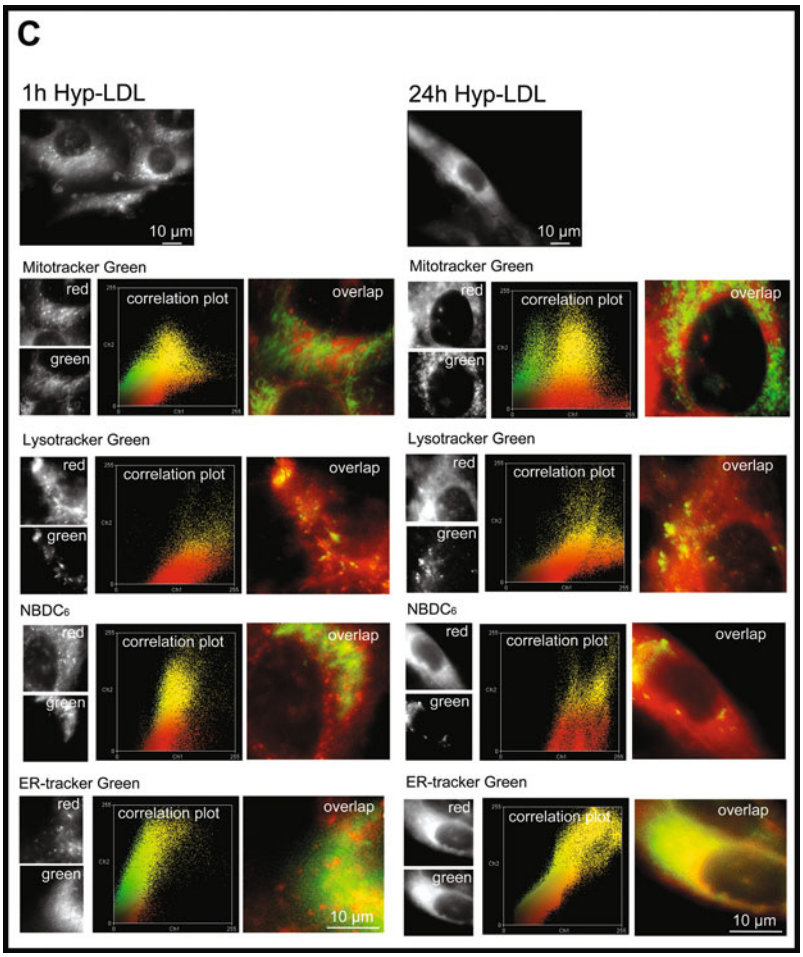

Fig. 3c Fluorescence images of U87 MG cells stained with specific fluorescent organelle probes (Mitotracker for mitochondria, Lysotracker for lysosomes, $NBDC_6$ for Golgi apparatus and ER-tracker for endoplasmic reticulum) were obtained after 1 h or 24 h incubation with the [Hyp–LDL] complex. Correlation plots between Hyp red fluorescence and green fluorescence of each organelle probe are given as well as corresponding overlap images.

aggregated).[41–43] In this view, further intracellular fluorescence lifetime measurements were performed for FRET assessment.

Fluorescence lifetime measurements

Taking into account the physical principle of FRET,[44] the decrease in the fluorescence lifetime of the donor molecule can only occur within a small distance between both molecules (less than ≈50 angstroms), which obviously can be considered as an optimal co-localization parameter. In order to give evidence of such FRET, the intracellular fluorescence lifetimes of Lysotracker Green were both measured in the absence, and presence of either Hyp or the [Hyp–LDL] complex (Fig. 4A). For a short incubation time (1 h), evidence of FRET in lysosomes is only given for cells treated with the [Hyp–LDL] complex, as shown by the observed decrease in the intracellular fluorescence lifetimes of Lysotracker Green (from 4.6 to 3.7 ns). Thus, on the contrary of what can be observed by the above fluorescence co-localization experiments, accumulation of Hyp in lysosomes, after 1 h incubation, is actually more pronounced in cells treated with the [Hyp–LDL] complex than for cells treated with free Hyp, but the aggregation process reduces its fluorescence. Obviously such a situation is more in agreement with the endocytosis pathway previously described for LDL.[45] In the same way, intracellular fluorescence lifetimes obtained with $NBDC_6$ (Fig. 4B) provides evidence that Hyp is actually accumulated in the Golgi apparatus (lifetime decrease from 6.2 to 3 and 4.4 ns for cells incubated with free Hyp and [Hyp–LDL] complex respectively). In view of these results the apparent opposite transfer of fluorescence observed in co-localization experiments should rather be interpreted as a consequence of aggregation processes consecutive to intracellular accumulation of Hyp. The following intracellular traffic can thus be suggest: For cells incubated with free Hyp, intracellular aggregation (or accumulation) first takes place at the mitochondrial level (after 1 h incubation) and then at the lysosomial level (6 h and 24 h incubation) while for cells incubated with the [Hyp–LDL] complex, aggregation first takes place in the lysosomes (1 h incubation) and then at the mitochondrial level. Nevertheless, if we take into account that the monomer fluorescent form of Hyp is the only photoactive form, the observed photo-induced cell death must be correlated with the actual intracellular fluorescent localization. From this point of view, the evolution of the photo-induced cell death as a function of the

Table 1 Co-localization analysis of organelle specific fluorescence probes with Hyp fluorescence in U87 glioma cells. M_{and} is Mandersons coefficient of co-localization (min. value 0, max. value 1). The M_{1Red} constant corresponds to the correlation of red pixels (Hyp fluorescence) of the image with the green pixels (organelle fluorescent probe): this constant displays the overlap coefficient of the fluorescent organelle probe with Hyp fluorescence. The M_{2Green} constant corresponds to the spatial overlap of green channel with red channel: it gives information about the relative presence of Hyp fluorescence in a given organelle

	Mitotracker® Green			Lysotracker® Green			$NBDC_6$			ERtracker® Green		
	M_{and}	M_{1Red}	M_{2Green}	M_{and}	M_{1Red}	M_{2Green}	M_{and}	M_{1Red}	M_{2Green}	M_{and}	M_{1Red}	M_{2Green}
Hyp												
1 h	0.56	0.42	1.00	0.78	**0.83**	1.00	0.52	0.30	1.00	0.92	**0.89**	0.99
24 h	0.91	**0.98**	0.99	0.66	0.62	1.00	0.42	0.14	1.00	0.87	**0.93**	1.00
Hyp–LDL												
1 h	0.88	**0.93**	0.99	0.67	0.53	1.00	0.71	0.49	1.00	0.92	**0.95**	0.99
24 h	0.68	0.79	0.97	0.81	**0.79**	1.00	0.57	0.33	1.00	0.96	**0.98**	1.00

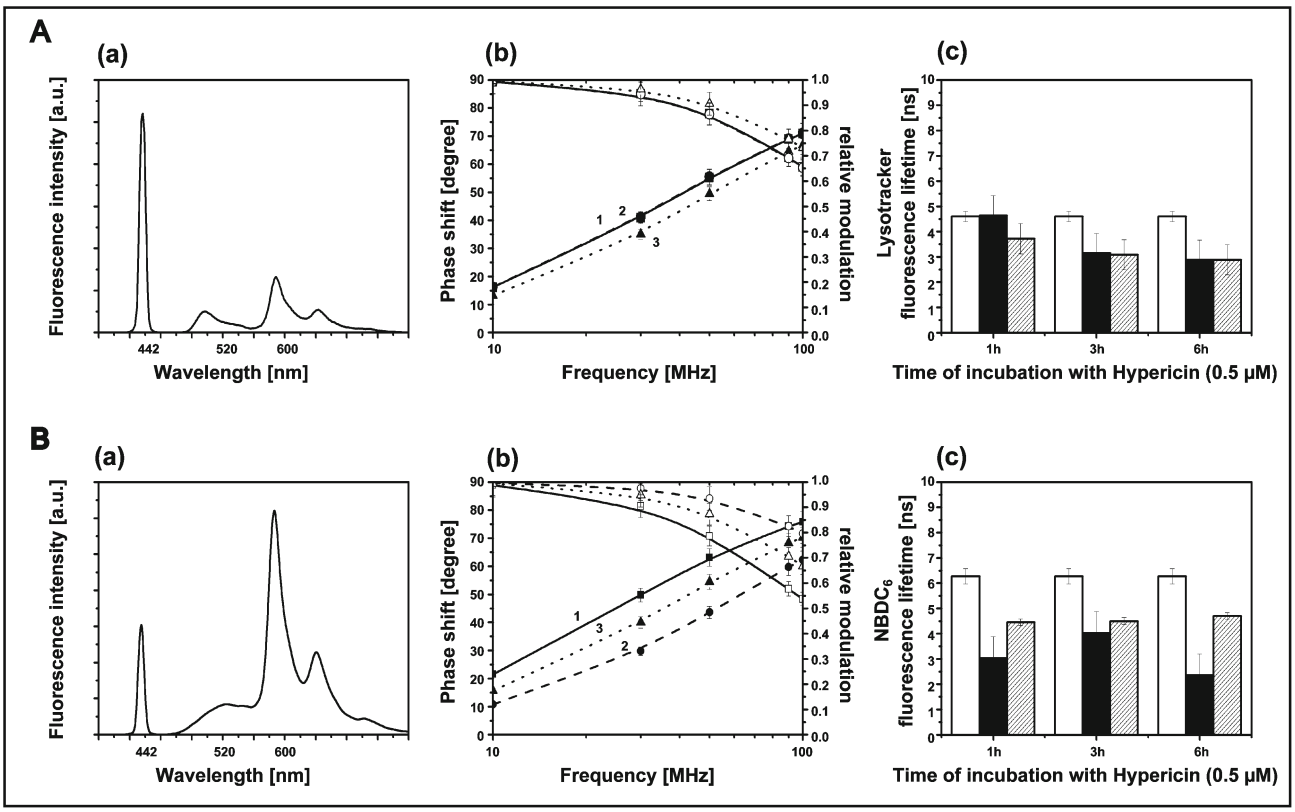

Fig. 4 Intracellular determination of organelle specific fluorescent lifetimes. Panel A corresponds to the determination of Lysotracker® Green DND-26 fluorescence lifetime and panel B corresponds to the determination of $NBDC_6$ fluorescence lifetime. (a) Characteristic intracellular fluorescent emission spectrum: diode laser excitation (maximum at 442 nm), green fluorescence of the probes (maximum around 510–520 nm) and red fluorescence of Hyp (maximum at 600 nm); (b) illustration of the frequency dependent phase shifts and relative modulations of the intracellular fluorescence of the probe that were measured in the absence of Hyp (curve 1) and after 1 h incubation with Hyp (curve 2) or the [Hyp–LDL] complex (curve 3). (c) Calculated intracellular fluorescence lifetimes of the probes as obtained without Hyp (□) or after 1 h, 3 h and 6 h of incubation with Hyp (■) or with the [Hyp–LDL] complex (▨).

incubation time (Fig. 1) clearly appears to be related to the evolution of the Hyp monomer localization in lysosomes (Fig. 3 and Table 1). Thus, we can consider that cell death photo-induced by low irradiation (4 J cm^{-2}) of U87 MG glioma cells after 1 to 24 h incubation with 500 nM Hyp is triggered at the lysosomial level. In view of this, the mitochondrial membrane depolarization, that can only be observed for cells incubated for 6 or 24 h incubation with the [Hyp–LDL] complex, should rather be considered as a consecutive effect of the primary photo-induced lysosomal damages, than as a consequence of direct mitochondrial photo-damage. Actually, the direct effect of the photo-activation of Hyp at the mitochondrial level can be observed in cells after 24 h incubation with free Hyp. In this case, fluorescence of the Hyp monomer is mainly localized in the mitochondria and not in the lysosomes. Accordingly, photo-activation leads to an hyper-polarization of the mitochondrial

membrane and to decreased cell death when compared to other cellular samples.

Conclusion

Due to possible aggregation processes and to dynamics of the intracellular traffic of Hyp, the incubation time before irradiation is a critical parameter that can affect the specific intracellular localization of its fluorescent monomer form. Since this monomer fluorescent form of Hyp is considered to be the only photoactive form, the dynamics of intracellular traffic also affects the photo-induced cell death pathway and should thus be carefully taken into consideration in view of PDT applications. Moreover, cellular delivery of Hyp, with LDLs that are considered as their natural vascular transport system, appears as an efficient way to increase the photo-induced cell death response. Dependence of Hyp uptake on different delivery systems, and related drug trafficking inside the cell forms the subject of our ongoing work.

Abbreviations

Hyp	hypericin
DMSO	dimethyl-sulfoxide
FRET	Fluorescence or Förster Resonant Energy Transfer
LDL	low-density lipoprotein
PDT	photodynamic therapy
Pts	photosensitizer

Acknowledgements

This work was supported by the (i) Agency of the Ministry of Education of Slovak Republic for the Structural funds of the European Union, Operational program Research and Development (Contracts: Doctorant, ITMS code: 26110230013) (50%) and NanoBioSens ITMS code: 26220220107 (50%) and by the International Program for Scientific Cooperation (PICS No. 5398) from the French National Center of Scientific Research (CNRS), (ii) Agency of the Ministry of Education of Slovak Republic project VEGA No 1/0241/09.

References

1 T. A. Theodossiou, J. S. Hothersall, P. A. De Witte, A. Pantos and P. Agostinis, The multifaceted photocytotoxic profile of hypericin, *Mol. Pharmaceutics*, 2009, **6**, 1775.
2 P. Miskovsky, Hypericin–a new antiviral and antitumor photosensitizer: mechanism of action and interaction with biological macromolecules, *Curr. Drug Targets*, 2002, **3**, 55.
3 P. Agostinis, A. Vantieghem, W. Merlevede and P. A. de Witte, Hypericin in cancer treatment: more light on the way, *Int. J. Biochem. Cell Biol.*, 2002, **34**, 221.
4 C. D. Cole, J. K. Liu, X. Sheng, S. S. Chin, M. H. Schmidt, M. H. Weiss and W. T. Couldwell, Hypericin-mediated photodynamic therapy of pituitary tumors: preclinical study in a GH4C1 rat tumor model, *J. Neuro-Oncol.*, 2008, **87**, 255.
5 D. Kacerovská, K. Pizinger, F. Majer and F. Smíd, Photodynamic therapy of nonmelanoma skin cancer with topical hypericum perforatum extract-A pilot study, *Photochem. Photobiol.*, 2008, **84**, 779.
6 A. Higuchi, E. H. Yamada, N. Jo Yamada and M. Matsumura, Hypericin inhibits pathological retinal neovascularization in a mouse model of oxygen-induced retinopathy, *Mol. Vis.*, 2008, **14**, 249.
7 A. R. Kamuhabwa, P. Agostinis, M. D'Hallewin, A. Kasran and P. A. de Witte, Photodynamic activity of hypericin in human urinary bladder carcinoma cells, *Anticancer Res.*, 2000, **20**, 2558.
8 J. C. Kah, W. K. Lau, P. H. Tan, C. J. Sheppard and M. Olivo, Endoscopic image analysis of photosensitizer fluorescence as a promising non-invasive approach for pathological grading of bladder cancer *in situ*, *J. Biomed. Opt.*, 2008, **13**, 054022.
9 R. Ritz, M. Müller, K. Dietz, F. Duffner, A. Borneman, F. Roser and M. Tatagiba, Hypericin uptake: a prognostic marker for survival in high-grade glioma, *J. Clin. Neurosci.*, 2008, **15**, 778.
10 T. A. Theodossiou, A. Noronha-Dutra and J. S. Hothersall, Mitochondria are a primary target of hypericin phototoxicity: synergy of intracellular calcium mobilisation in cell killing, *Int. J. Biochem. Cell Biol.*, 2006, **38**, 1946.
11 S. M. Ali and M. Olivo, Bio-distribution and subcellular localization of Hypericin and its role in PDT induced apoptosis in cancer cells, *Int. J. Oncol.*, 2002, **21**, 531.
12 C. Thomas and R. S. Pardini, Oxygen dependence of hypericin-induced phototoxicity to EMT6 mouse mammary carcinoma cells, *Photochem. Photobiol.*, 1992, **55**, 831.
13 P. Miskovsky, F. Sureau, L. Chinsky and P. Y. Turpin, Subcellular distribution of hypericin in human cancer cells, *Photochem. Photobiol.*, 1995, **62**, 546.
14 A. L. Vandenbogaerte, J. F. Cuveele, P. B. E. Himpens, W. J. Merlevede and P. A. de Witte, Differencial cytotoxic effects induced after photosensitization of hypericin, *J. Photochem. Photobiol., B*, 1997, **38**, 136.
15 A. L. Vandenbogaerte, A. Kamuhabwa, E. Delaey, B. E. Himpens, W. J. Merlevede and P. A. de Witte, Phototoxic effect of pseudohypericin *versus* hypericin, *J. Photochem. Photobiol., B*, 1998, **45**, 87.
16 A. L. Vandenbogaerte, E. Delaey and A. M. Vantienghem, Cytotoxicity and antiproliferative effect of hypericin and derivatives after photosensitization, *Photochem. Photobiol.*, 1998, **67**, 119.
17 R. Ritz, F. Roser, N. Radomski, W. S. Straus, M. Tatagiba and A. Gharabaghi, Subcellular colocalization of hypericin with respect to endoplasmic reticulum and Golgi apparatus in glioblastoma cells, *Anticancer Res.*, 2008, **28**, 2033.
18 A. B. Uzdensky, L. W. Ma, V. Iani, G. O. Hjortland, H. B. Steen and J. Moan, J. Intracellular localization of hypericin in human glioblastoma and carcinoma cell lines, *Lasers Med. Sci.*, 2001, **16**, 276.
19 S. Kascakova, Z. Nadova, A. Mateasik, J. Mikes, V. Huntosova, M. Refregier, F. Sureau, J. C. Maurizot, P. Miskovsky and D. Jancura, High level of low-density lipoprotein receptors enhance hypericin uptake by U-87 MG cells in the presence of LDL, *Photochem. Photobiol.*, 2008, **84**, 120.
20 G. Pfaffel-Schubart, A. Ruck and C. Scalfi-Happ, Modulation of cellular Ca2+-signaling during hypericin-induced photodynamic therapy (PDT), *Med. Laser Appl.*, 2006, **21**, 61.
21 D. R. Green and J. C. Reed, Mitochondria and apoptosis, *Science*, 1998, **281**, 1309.
22 Y. F. Ho, M. H. Wu, B. H. Cheng, Y. W. Chen and M. C. Shih, Lipid-mediated preferential localization of hypericin in lipid membranes, *Biochim. Biophys. Acta*, 2009, **1788**, 1287.
23 V. Huntosova, L. Alvarez, L. Bryndzova, Z. Nadova, D. Jancura, L. Buriankova, S. Bonneau, D. Brault, P. Miskovsky and F. Sureau, Interaction dynamics of hypericin with low-density lipoproteins and U87-MG cells, *Int. J. Pharm.*, 2010, **389**, 32.
24 R. Ritz, H. T. Wein, K. Dietz, M. Schenk, F. Roser, M. Tatagiba and W. S. Strauss, Photodynamic therapy of malignant glioma with hypericin: comprehensive *in vitro* study in human glioblastoma cell lines, *Int. J. Oncol.*, 2007, **30**, 659.
25 T. Theodossiou, M. D. Spiro, J. Jacobson, J. S. Hothersall and A. J. Macrobert, Evidence for intracellular aggregation of hypericin and the impact on its photocytotoxicity in PAM 212 murine keratinocytes, *Photochem. Photobiol.*, 2004, **80**, 438.
26 B. A. Allison, P. H. Pritchard and J. G. Levy, Evidence for low-density lipoprotein receptor-mediated uptake of benzoporphyrin derivative, *Br. J. Cancer*, 1995, **69**, 833.
27 R. A. Firestone, Low-density lipoprotein as a vehicle for targeting antitumor compounds to cancer cells, *Bioconjugate Chem.*, 1994, **5**, 105.
28 L. Maletinska, E. A. Blakely, K. A. Bjornstand, D. F. Deen, L. J. Knoff and T. M. Forte, Human glioblastoma cell lines: levels of Low-density lipoprotein receptor and low-density lipoprotein receptor-related protein, *Cancer Res.*, 2000, **60**, 2300.
29 S. Kascakova, M. Refregiers, D. Jancura, F. Sureau, J. C. Maurizot and P. Miskovsky, Fluorescence spectroscopic study of hypericin-

photosensitized oxidation of low-density lipoproteins, *Photochem. Photobiol.*, 2005, **81**, 1395.
30 P. Gbur, R. Dedic, D. Chorvat, P. Miskovsky, J. Hala and D. Jancura, Time-resolved luminescence and singlet oxygen formation after illumination of the hypericin-low-density lipoprotein complex, *Photochem. Photobiol.*, 2009, **85**, 816.
31 P. Mukherjee, R. Adhikary, M. Halder, J. W. Petrich and P. Miskovsky, Accumulation and interaction of hypericin in low-density lipoprotein – a photophysical study, *Photochem. Photobiol.*, 2008, **84**, 706.
32 G. Lajos, D. Jancura, P. Miskovsky, J. V. G. Ramos and S. S. Cortez, Interaction of the photosensitizer hypericin with low-density lipoproteins and phosphatidylcholine: a surface-enhanced Raman scattering and surface-enhanced fluorescence study, *J. Phys. Chem. C*, 2009, **113**, 7147.
33 L. Buriankova, D. Buzova, D. Chorvat Jr., F. Sureau, D. Brault and P. Miskovsky, Kinetics of hypericin association with low-density lipoproteins, *Photochem. Photobiol.*, 2011, **87**, 56.
34 E. Mille, Apoptosis measurement by Annexin V staining, *Methods Mol. Med.*, 2004, **88**, 191.
35 H. Rottenberg and S. Wu, Quantitative assay by flow cytometry of the mitochondrial membrane potential in intact cells, *Biochim. Biophys. Acta*, 1998, **1404**, 393.
36 E. E. M. Manders, F. J. Verbeek and J. A. Aten, Measurement of co-localisation of objects in dual-colour confocal images, *J. Microsc.*, 1993, **169**, 375.
37 S. Bolte and F. P. Cordelieres, A guided tour into subcellular colocalization analysis in light microscopy, *J. Microsc.*, 2006, **224**, 213.
38 J. Boutet de Monvel, E. Scarfone, S. Le Calves and M. Ulfendahl, Image-adaptative deconvolution for three-dimensional deep biological imaging, *Biophys. J.*, 2003, **85**, 3991.
39 K. Suhling, P. M. French and D. Phillips, Time-resolved fluorescence microscopy, *Photochem. Photobiol. Sci.*, 2005, **4**, 13.
40 J. J. Reiners Jr., J. A. Caruso, P. Mathieu, B. Chelladurai, X. M. Yin and D. Kessel, Release of cytochrome *c* and activation of pro-caspase-9 following lysosomal photodamage involves Bid cleavage, *Cell Death Differ.*, 2002, **9**, 934.
41 A. Vantieghem, Z. Assefa, P. Vandenabeele, W. Declercq, S. Courtois, J. R. Vandenheede, W. Merlevede, P. de Witte and P. Agostinis, Hypericin-induced photosensitization of HeLa cells leads to apoptosis or necrosis. Involvement of cytochrome *c* and procaspase-3 activation in the mechanism of apoptosis, *FEBS Lett.*, 1998, **440**, 19.
42 L. W. Runnels and S. F. Scarlata, Theory and application of fluorescence homotransfer to melittin oligomerization, *Biophys. J.*, 1995, **69**, 1569.
43 R. F. Chen and J. R. Knutson, Mechanism of fluorescence concentration quenching of carboxyfluorescein in liposomes: energy transfer to nonfluorescent dimmers, *Anal. Biochem.*, 1988, **172**, 61.
44 J. R. Lakowicz, *Principles of Fluorescence Spectroscopy*, 2nd edn, Springer, Germany, 1999, ch. 13.1, pp. 368–373.
45 M. S. Brown, Y. K. Ho and J. L. Goldstein, The low-density lipoprotein pathway in human fibroblasts: relation between cell surface receptor binding and endocytosis of low-density lipoprotein, *Ann. N. Y. Acad. Sci.*, 1976, **275**, 244.

